22

Alloys

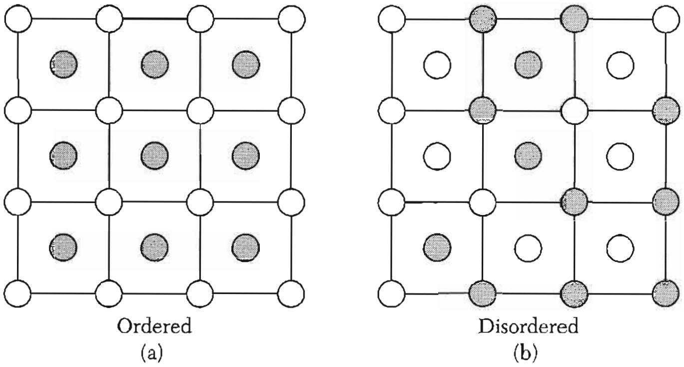
Ordered
(a)

Disordered
(b)

Figure 1 Ordered (a) and disordered (b) arrangements of AB ions in the alloy AB.

CHAPTER 22: ALLOYS

GENERAL CONSIDERATIONS

The theory of the band structure of solids assumes that the crystal has translational invariance. But suppose that the crystal is composed of two elements A and B that occupy at random the regular lattice sites of the structure, in proportions x and $1 - x$ for the composition A_xB_{1-x}. The translational symmetry is no longer perfect. Will we then lose the consequences of band theory, such as the existence of Fermi surfaces and of energy gaps? Will insulators become conductors because the energy gap is gone? We touched on these questions in the discussion of amorphous semiconductors in Chapter 19.

Experiment and theory agree that the consequences of the destruction of perfect translational symmetry are much less serious (nearly always) than we expect at first sight. The viewpoint of the effective screened potential of Chapter 9 is helpful in these matters, first because the effective potentials are relatively weak in comparison with a free ion potential and, second and most important, the differences between the effective potentials of the host and the additive atoms may be very weak in comparison with either alone. Alloys of Si and Ge or of Cu and Ag are classic examples of what we may call the relative ineffectiveness of alloying.

In any event, a low concentration of impurity atoms cannot have much effect on the Fourier components $U_{\mathbf{G}}$ of the effective potential $U(\mathbf{r})$ that is responsible for the band gaps and for the form of the Fermi surface. (This statement implies that the **G**'s exist, which implies that a regular lattice exists. This is not an important assumption because we know that thermal phonons do not have drastic effects on the band structure, so that lattice distortions described as frozen-in phonons should not have drastic effects. If the distortions are more serious, as with amorphous solids, the electronic changes can be significant.)

It is true that an impurity atom will introduce Fourier components of $U(\mathbf{r})$ at wavevectors that are not reciprocal lattice vectors, but at low impurity concentration such components are never large in comparison with the $U_{\mathbf{G}}$, arguing from the statistics of random potentials. The Fourier components at the reciprocal lattice vectors **G** will still be large and will give the band gaps, Fermi surfaces, and sharp x-ray diffraction lines characteristic of a regular lattice.

The consequences of alloying will be particularly small when the impurity element belongs to the same column of the periodic table as the host element it replaces, because the atomic cores will make rather similar contributions to the effective potentials.

One measure of the effect of alloying is the residual electrical resistivity, defined as the low temperature limit of the resistivity. Here we must distinguish

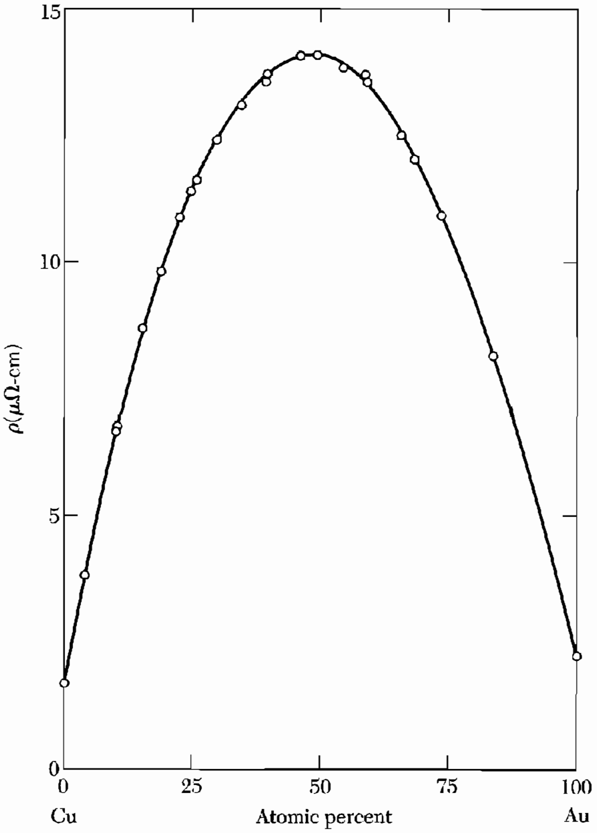

Figure 2 Resistivity of a disordered binary alloy of copper and gold. The variation of the residual resistivity depends on the composition Cu_xAu_{1-x} as $x(1-x)$, which is known as Nordheim's Rule for a disordered alloy. Here $x(1-x)$ is a measure of the degree of maximum disorder possible for a given value of x. (Johansson and Linde.)

between disordered and ordered alloys. An alloy is disordered if the A and B atoms are randomly arranged, which occurs for a general value of x in the composition A_xB_{1-x}. For special values of x, such as 1/4, 1/2, and 3/4 for a cubic structure, it is possible for ordered phases to form, phases in which the A and B atoms form an ordered array. The distinction between order and disorder is shown in Fig. 1. The effect of order on the electrical resistivity is shown in Figs. 2 and 3. The residual resistivity increases with disorder, as discussed for amorphous materials in Chapter 19. The effect is shown in Fig. 2 for the Cu-Au alloy system. When the specimen is cooled slowly from a high temperature, ordered structures are formed at Cu_3Au and CuAu; these structures have a lower residual resistivity by virtue of their order, as in Fig. 3.

Thus we can use the residual electrical resistivity to measure the effect of alloying in a disordered structure. One atomic percent of copper dissolved in silver (which lies in the same column of the periodic table) increases the

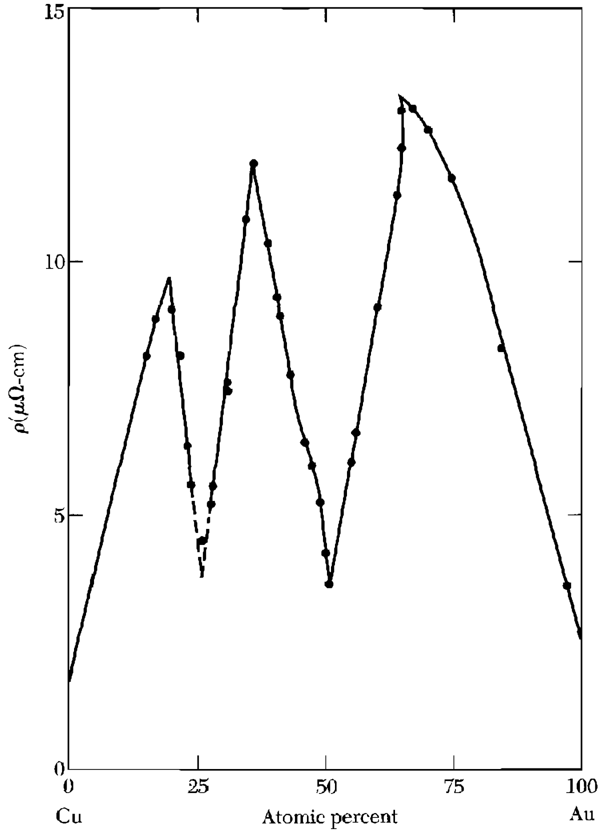

Figure 3 Effect of ordered phases on the resistivity of a binary alloy Cu_xAu_{1-x}. The alloys here have been annealed, whereas those in Fig. 2 have been quenched (cooled rapidly). The compositions of low residual resistivity correspond to the ordered compositions Cu_3Au and CuAu. (Johansson and Linde.)

residual resistivity by 0.077 μohm-cm. This corresponds to a geometrical scattering cross section which is only 3 percent of the naive "projected area" of the impurity atom, so that the scattering effect is very small.

In insulators there is no experimental evidence for a significant reduction of band gap caused by the random potential components. For example, silicon and germanium form homogeneous solid solutions, known as substitutional alloys, over the entire composition range, but the band edge energies vary continuously with composition from the pure Si gap to the pure Ge gap.

It is widely believed, however, that the density of states near the band edges in amorphous materials is smeared by the gross absence of translational symmetry. Some of the new states thus formed just inside the gap may not necessarily be current-carrying states because they may not extend throughout the crystal.

SUBSTITUTIONAL SOLID SOLUTIONS—HUME-ROTHERY RULES

We now discuss substitutional solid solutions of one metal A in another metal B of different valence, where A and B occupy, at random, equivalent sites in the structure. Hume-Rothery treated the empirical requirements for the stability of a solid solution of A and B as a single phase system.

One requirement is that the atomic diameters be compatible, which means that they should not differ by more than 15 percent. For example, the diameters are favorable in the Cu (2.55 Å) – Zn (2.65 Å) alloy system: zinc dissolves in copper as an fcc solid solution up to 38 atomic percent zinc. The diameters are less favorable in the Cu (2.55 Å) – Cd (2.97 Å) system, where only 1.7 atomic percent cadmium is soluble in copper. The atomic diameters referred to copper are 1.04 for zinc and 1.165 for cadmium.

Although the atomic diameters may be favorable, solid solutions will not form when there is a strong chemical tendency for A and B to form "intermetallic compounds," which are compounds of definite chemical proportions. If A is strongly electronegative and B strongly electropositive, compounds such as AB and A_2B may precipitate from the solid solution. (This is different from the formation of an ordered alloy phase only by the greater chemical bonding strength of the intermetallic compounds.) Although the atomic diameter ratio is favorable for As in Cu (1.02), only 6 atomic percent As is soluble. The diameter ratio is also favorable for Sb in Mg (1.06), yet the solubility of Sb in Mg is very small.

The electronic structure of alloys can often be described by the average number of conduction electrons (or valence electrons) per atom, denoted by n. In the alloy CuZn the value of n is 1.50; in CuAl, $n = 2.00$. Changes in electron concentration determine structural changes in many alloy systems.

The phase diagram of the copper-zinc system[1] is shown in Fig. 4. The fcc structure of pure copper ($n = 1$) persists on the addition of zinc ($n = 2$) until the electron concentration reaches 1.38. A bcc structure occurs at a minimum electron concentration of about 1.48. The γ phase exists for the approximate range of n between 1.58 and 1.66, and the hcp phase ϵ occurs near 1.75.

The term **electron compound** denotes an intermediate phase (such as the β phase of CuZn) whose crystal structure is determined by a fairly well defined electron to atom ratio. For many alloys the ratio is close to the **Hume-Rothery rules**: 1.50 for the β phase, 1.62 for the γ phase, and 1.75 for the ϵ phase. Representative experimental values are collected in Table 1, based on the usual chemical valence of 1 for Cu and Ag; 2 for Zn and Cd; 3 for Al and Ga; 4 for Si, Ge, and Sn.

The Hume-Rothery rules find a simple expression in terms of the band theory of nearly free electrons. The observed limit of the fcc phase occurs

---

[1] The phases of interest are usually denoted by metallurgists by Greek characters: in the Cu-Zn system we have α (fcc), β (bcc), γ (complex cubic cell of 52 atoms), ϵ (hcp) and η (hcp); ϵ and η differ considerably in c/a ratio. The meaning of the characters depends on the alloy system.

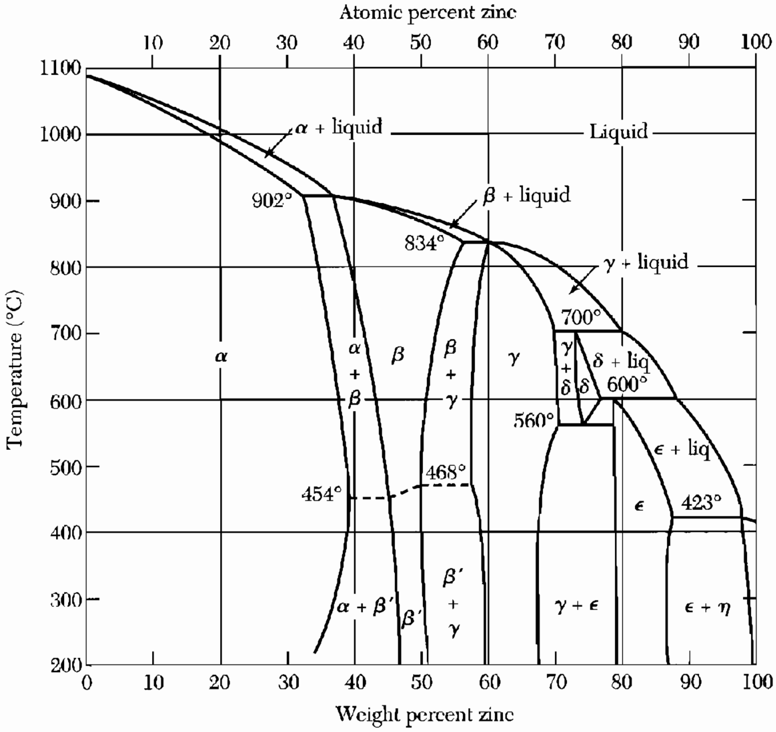

Figure 4 Equilibrium diagram of phases in the copper-zinc alloy system. The α phase is fcc; β and β' are bcc; γ is a complex structure; ϵ and η are both hcp, but ϵ has a c/a ratio near 1.56 and η (for pure Zn) has $c/a = 1.86$. The β' phase is ordered bcc, by which we mean that most of the Cu atoms occupy sites on one sc sublattice and most of the Zn atoms occupy sites on a second sc sublattice that interpenetrates the first sublattice. The β phase is disordered bcc: any site is equally likely to be occupied by a Cu or Zn atom, almost irrespective of what atoms are in the neighboring sites.

Table 1 Electron/atom ratios of electron compounds

Alloy	fcc phase boundary	Minimum bcc phase boundary	γ-phase boundaries	hcp phase boundaries
Cu-Zn	1.38	1.48	1.58–1.66	1.78–1.87
Cu-Al	1.41	1.48	1.63–1.77	
Cu-Ga	1.41			
Cu-Si	1.42	1.49		
Cu-Ge	1.36			
Cu-Sn	1.27	1.49	1.60–1.63	1.73–1.75
Ag-Zn	1.38		1.58–1.63	1.67–1.90
Ag-Cd	1.42	1.50	1.59–1.63	1.65–1.82
Ag-Al	1.41			1.55–1.80

close to the electron concentration of 1.36 at which an inscribed Fermi sphere makes contact with the Brillouin zone boundary for the fcc lattice. The observed electron concentration of the bcc phase is close to the concentration 1.48 at which an inscribed Fermi sphere makes contact with the zone boundary for the bcc lattice. Contact of the Fermi sphere with the zone boundary for the γ phase is at the concentration 1.54. Contact for the hcp phase is at the concentration 1.69 for the ideal c/a ratio.

Why is there a connection between the electron concentrations at which a new phase appears and at which the Fermi surface makes contact with the boundary of the Brillouin zone? We recall that the energy bands split into two at the region of contact on the zone boundary (Chapter 9). If we add more electrons to the alloy at this stage, they will have to be accommodated in the upper band or in states of high energy near the zone corners of the lower band. Both options are possible, and both involve an increase of energy. It may also be energetically favorable for the crystal structure to change to one which can contain a Fermi surface of larger volume (more electrons) before contact is made with the zone boundary. In this way H. Jones made plausible the sequence of structures fcc, bcc, γ, hcp with increasing electron concentration.

Measurements of the lattice parameter of Li-Mg alloys are shown in Fig. 5. In the range shown the structure is bcc. The lattice contracts during the initial stages of the addition of Mg to Li. When the lithium content drops below 50 atomic percent, corresponding to an average electron concentration increasing above 1.5 per atom, the lattice starts to expand. We have seen that

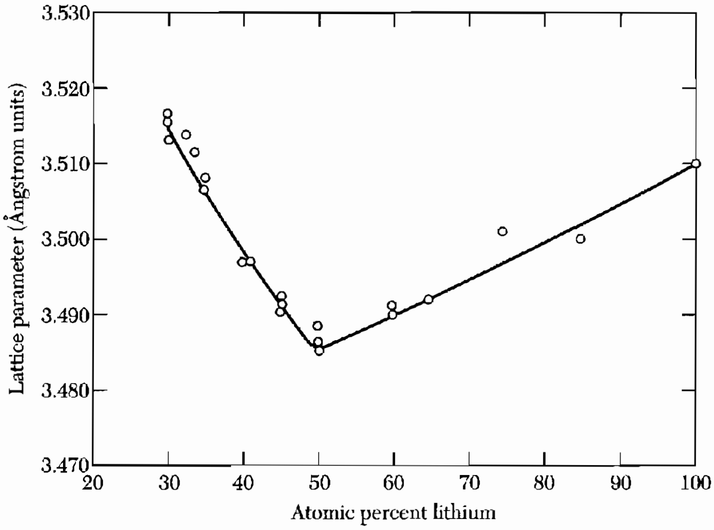

Figure 5 Lattice parameter of body-centered cubic magnesium-lithium alloys. (After D. W. Levinson.)

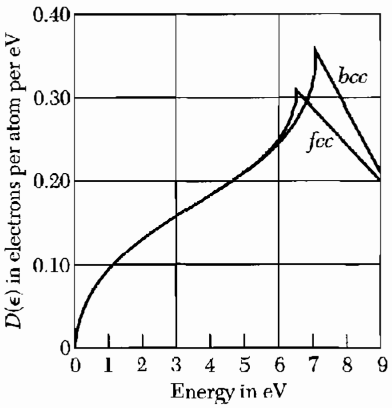

Figure 6 Number of orbitals per unit energy range for the first Brillouin zone of the fcc and bcc lattices, as a function of energy.

for a spherical Fermi surface, contact with the zone boundary is established at $n = 1.48$ electrons per atom, in a bcc lattice. It appears that the expansion of the lattice arises from the onset of overlap across the zone boundary.

The transformation from fcc to bcc is illustrated by Fig. 6; this shows the number of orbitals per unit energy range as a function of energy, for the fcc and bcc structures. As the number of electrons is increased, a point is reached where it is easier to accommodate additional electrons in the Brillouin zone of the bcc lattice rather than in the Brillouin zone of the fcc lattice. The figure is drawn for copper.

ORDER-DISORDER TRANSFORMATION

The dashed horizontal line in the beta-phase (bcc) region of the phase diagram (Fig. 4) of the Cu-Zn system represents the transition temperature between the ordered (low temperature) and disordered (high temperature) states of the alloy. In the common ordered arrangement of an AB alloy with a bcc structure, all the nearest-neighbor atoms of a B atom are A atoms, and vice versa. This arrangement results when the dominant interaction among the atoms is an attraction between A and B atoms. (If the AB interaction is weakly attractive or repulsive, a two-phase system is formed in which some crystallites are largely A and other crystallites are largely B.)

The alloy is completely ordered in equilibrium at absolute zero. It becomes less ordered as the temperature is increased, until a transition temperature is reached above which the structure is disordered. The transition temperature marks the disappearance of **long-range order**, which is order over many interatomic distances, but some **short-range order** or correlation among near neighbors may persist above the transition. The long-range order in an AB alloy is shown in Fig. 7a. Long- and short-range order for an alloy of composition AB_3 is given in Fig. 7b. The degree of order is defined below.

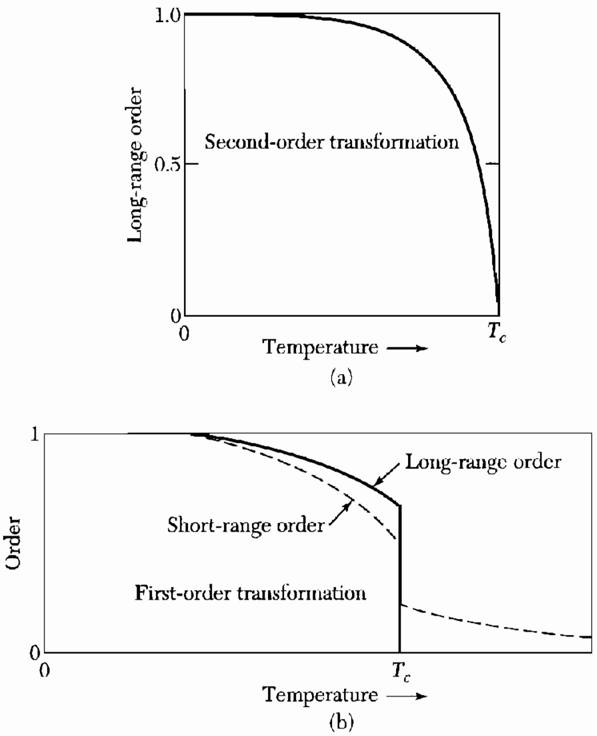

Figure 7 (a) Long-range order versus temperature for an AB alloy. The transformation is second order. (b) Long-range and short-range order for an AB_3 alloy. The transformation for this composition is first order.

If an alloy is cooled rapidly from high temperatures to a temperature below the transition, a metastable condition may be produced in which a nonequilibrium disorder is frozen in the structure. The reverse effect occurs when an ordered specimen is disordered at constant temperature by heavy irradiation with nuclear particles. The degree of order may be investigated experimentally by x-ray diffraction. The disordered structure in Fig. 8 has diffraction lines at the same positions as if the lattice points were all occupied by only one type of atom, because the effective scattering power of each plane is equal to the average of the A and B scattering powers. The ordered structure has extra diffraction lines not possessed by the disordered structure. The extra lines are called **superstructure lines**.

The use of the terms order and disorder in this chapter always refers to regular lattice sites; it is the occupancy that is randomly A or B. Do not confuse this usage with that of Chapter 19 on noncrystalline solids where there are no regular lattice sites and the structure itself is random. Both possibilities occur in nature.

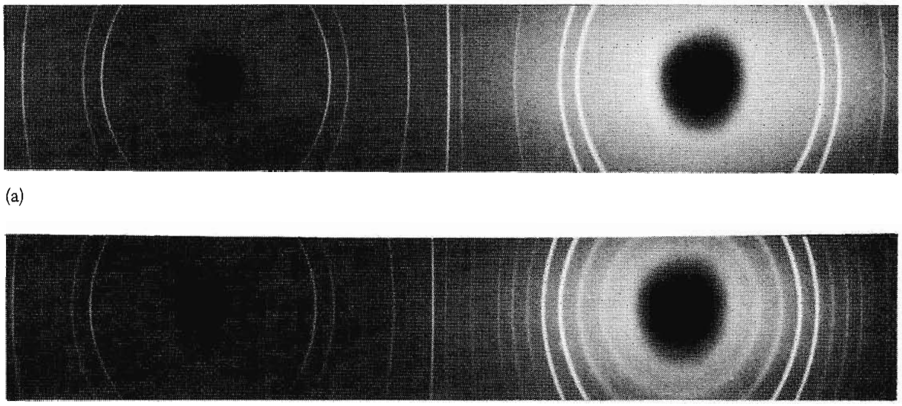

(a)

(b)

Figure 8 X-ray powder photographs in $AuCu_3$ alloy. (a) Disordered by quenching from $T > T_c$; (b) ordered by annealing at $T < T_c$. (Courtesy of G. M. Gordon.)

The structure of the ordered CuZn alloy is the cesium chloride structure of Chapter 1. The space lattice is simple cubic, and the basis has one Cu atom at 000 and one Zn atom at $\frac{1}{2}\frac{1}{2}\frac{1}{2}$. The diffraction structure factor

$$S(hkl) = f_{Cu} + f_{Zn}\, e^{-i\pi(h+k+l)} \quad . \tag{1}$$

This cannot vanish because $f_{Cu} \neq f_{Zn}$; therefore all reflections of the simple cubic space lattice will occur. In the disordered structure the situation is different: the basis is equally likely to have either Zn or Cu at 000 and either Zn or Cu at $\frac{1}{2}\frac{1}{2}\frac{1}{2}$. Then the average structure factor is

$$\langle S(hkl) \rangle = \langle f \rangle + \langle f \rangle\, e^{-i\pi(h+k+l)} \quad , \tag{2}$$

where $\langle f \rangle = \frac{1}{2}(f_{Cu} + f_{Zn})$. Equation (2) is exactly the form of the result for the bcc lattice; the reflections vanish when $h + k + l$ is odd. We see that the ordered lattice has reflections (the superstructure lines) not present in the disordered lattice (Fig. 8).

Elementary Theory of Order

We give a simple statistical treatment of the dependence of order on temperature for an AB alloy with a bcc structure. The case A_3B differs from AB, the former having a first-order transition marked by a latent heat and the latter having a second-order transition marked by a discontinuity in the heat capacity (Fig. 9). We introduce a measure of the long-range order. We call one simple cubic lattice a and the other b: the bcc structure is composed of the two interpenetrating sc lattices, and the nearest neighbors of an atom on one lattice lie on the other lattice. If there are N atoms A and N atoms B in the alloy, the

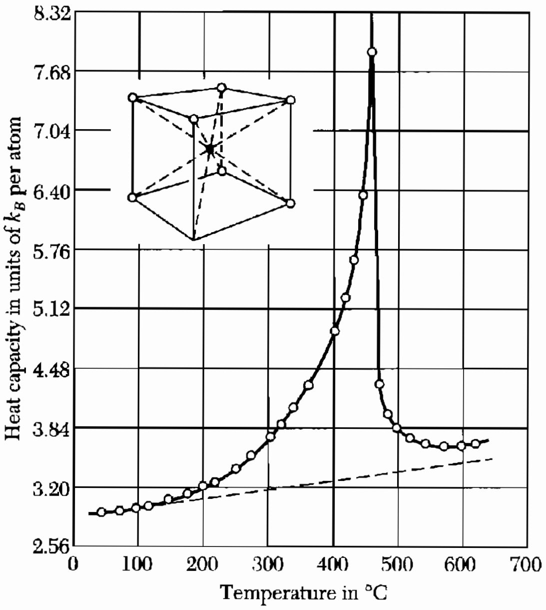

Figure 9 Heat capacity versus temperature of CuZn alloy (β-brass).

long-range order parameter P is defined so that the number of A's on the lattice a is equal to $\frac{1}{2}(1 + P)N$. The number of A's on lattice b is equal to $\frac{1}{2}(1-P)N$. When $P = \pm 1$, the order is perfect and each lattice contains only one type of atom. When $P = 0$, each lattice contains equal numbers of A and B atoms and there is no long-range order.

We consider that part of the internal energy associated with the bond energies of AA, AB, and BB nearest-neighbor pairs. The total bond energy is

$$E = N_{AA}U_{AA} + N_{BB}U_{BB} + N_{AB}U_{AB} \ , \tag{3}$$

where N_{ij} is the number of nearest-neighbor ij bonds and U_{ij} is the energy of an ij bond.

The probability that an atom A on lattice a will have an AA bond is equal to the probability that an A occupies a particular nearest-neighbor site on b, times the number of nearest-neighbor sites, which is 8 for the bcc structure. We assume that the probabilities are independent. Thus, by the preceding expressions for the number of A's on a and b,

$$\begin{aligned} N_{AA} &= 8[\tfrac{1}{2}(1 + P)N][\tfrac{1}{2}(1 - P)] = 2(1 - P^2)N \ ; \\ N_{BB} &= 8[\tfrac{1}{2}(1 + P)N][\tfrac{1}{2}(1 - P)] = 2(1 - P^2)N \ ; \\ N_{AB} &= 8N[\tfrac{1}{2}(1 + P)]^2 + 8N[\tfrac{1}{2}(1 - P)]^2 = 4(1 + P^2)N \ . \end{aligned} \tag{4}$$

The energy (3) becomes

$$E = E_0 + 2NP^2U \ , \tag{5}$$

where

$$E_0 = 2N(U_{AA} + U_{BB} + 2U_{AB}) \ ; \qquad U = 2U_{AB} - U_{AA} - U_{BB} \ . \tag{6}$$

We now calculate the entropy of this distribution of atoms. There are $\frac{1}{2}(1 + P)N$ atoms A and $\frac{1}{2}(1 - P)N$ atoms B on lattice a; there are $\frac{1}{2}(1 - P)N$ atoms A and $\frac{1}{2}(1 + P)N$ atoms B on lattice b. The number of arrangements G of these atoms is

$$G = \left[\frac{N!}{[\frac{1}{2}(1 + P)N]![\frac{1}{2}(1 - P)N]!} \right]^2 \ . \tag{7}$$

From the definition of the entropy as $S = k_B \ln G$, we have, using Stirling's approximation,

$$S = 2Nk_B \ln 2 - Nk_B[(1 + P)\ln(1 + P) + (1 - P)\ln(1 - P)] \ . \tag{8}$$

This defines the **entropy of mixing**. For $P = \pm 1$, $S = 0$; for $P = 0$, $S = 2Nk_B \ln 2$.

The equilibrium order is determined by the requirement that the free energy $F = E - TS$ be a minimum with respect to the order parameter P. On differentiating F with respect to P, we have as the condition for the minimum

$$4NPU + Nk_BT \ln \frac{1 + P}{1 - P} = 0 \ . \tag{9}$$

The transcendental equation for P may be solved graphically; we find the smoothly decreasing curve shown in Fig. 7a. Near the transition we may expand (9) to find $4NPU + 2Nk_BTP = 0$. At the transition temperature $P = 0$, so that

$$T_c = -2U/k_B \ . \tag{10}$$

For a transition to occur, the effective interaction U must be negative.

The **short-range order parameter** r is a measure of the fraction of the average number q of nearest-neighbor bonds that are AB bonds. When completely disordered, an AB alloy has an average of four AB bonds about each atom A. The total possible is eight. We may define

$$r = \frac{1}{4}(q - 4) \ , \tag{11}$$

so that $r = 1$ in complete order and $r = 0$ in complete disorder. Observe that r is a measure only of the local order about an atom, whereas the long-range order parameter P refers to the purity of the entire population on a given sublattice. Above the transition temperature T_c the long-range order is rigorously zero, but the short-range order is not.

PHASE DIAGRAMS

There is a large amount of information in a phase diagram even for a binary system, as in Fig. 4. The areas enclosed by curves relate to the equilibrium state in that region of composition and temperature. The curves mark the course of phase transitions as plotted in the T-x plane, where x is the composition parameter.

The equilibrium state is the state of minimum free energy of the binary system at given T, x. Thus the analysis of a phase diagram is the subject of thermodynamics. Several extraordinary results come out of this analysis, in particular the existence of low-melting-point eutectic compositions. Because the analysis has been treated in Chapter 11 of *TP*, we only outline the principal results here.

Two substances will dissolve in each other and form a homogeneous mixture if that is the configuration of lowest free energy accessible to the components. The substances will form a heterogeneous mixture if the combined free energy of the two separate phases side by side is lower than the free energy of the homogeneous mixture. Now we say that the mixture exhibits a **solubility gap**. In Fig. 4 we see that compositions near $Cu_{0.60}Zn_{0.40}$ are in a solubility gap and are mixtures of fcc and bcc phases of different structures and compositions. The phase diagram represents the temperature dependence of the solubility gaps.

When a small fraction of a homogeneous liquid freezes, the composition of the solid that forms is almost always different from that of the liquid. Consider a horizontal section near the composition $Cu_{0.80}Zn_{0.20}$ in Fig. 4. Let x denote the weight percent of zinc. At a given temperature, there are three regions:

$x > x_L$, the equilibrium system is a homogeneous liquid.
$x_S < x < x_L$, there is a solid phase of composition x_S and a liquid phase of composition x_L.
$x < x_S$, equilibrium system is a homogeneous solid.

The point x_L traces a curve called the **liquidus** curve, and the point x_S traces the **solidus** curve.

Eutectics. Mixtures with two liquidus branches in their phase diagram are called eutectics, as in Fig. 10 for the Au-Si system. The minimum solidification temperature is called the eutectic temperature; here the composition is the eutectic composition. The solid at this composition consists of two separate phases, as in the microphotograph of Fig. 11.

There are many binary systems in which the liquid phase persists to temperatures below the lower melting temperature of the constituents. Thus $Au_{0.69}Si_{0.31}$ solidifies at 370°C as a two-phase heterogeneous mixture, although Au and Si solidify at 1063°C and 1404°C, respectively. One phase of the eutectic is nearly pure gold; the other nearly pure silicon.

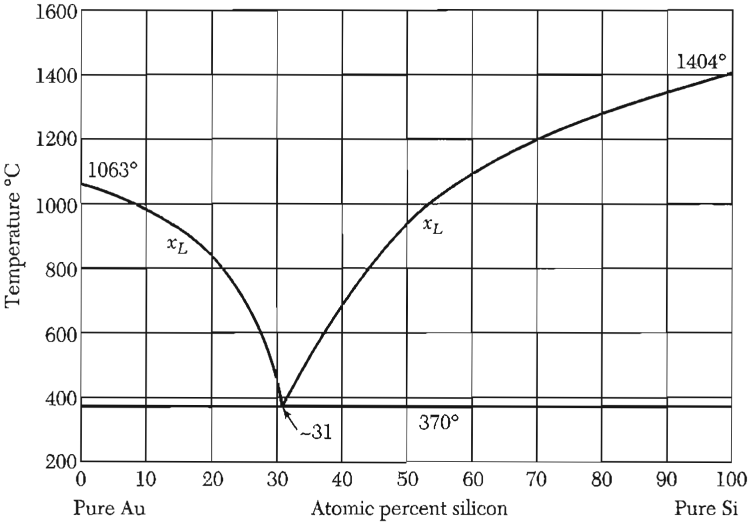

Figure 10 Eutectic phase diagram of gold-silicon alloys. The eutectic consists of two branches that come together at T_c = 370 °C and x_g = 0.31 atomic percent Si. (After Kittel and Kroemer, *TP*.)

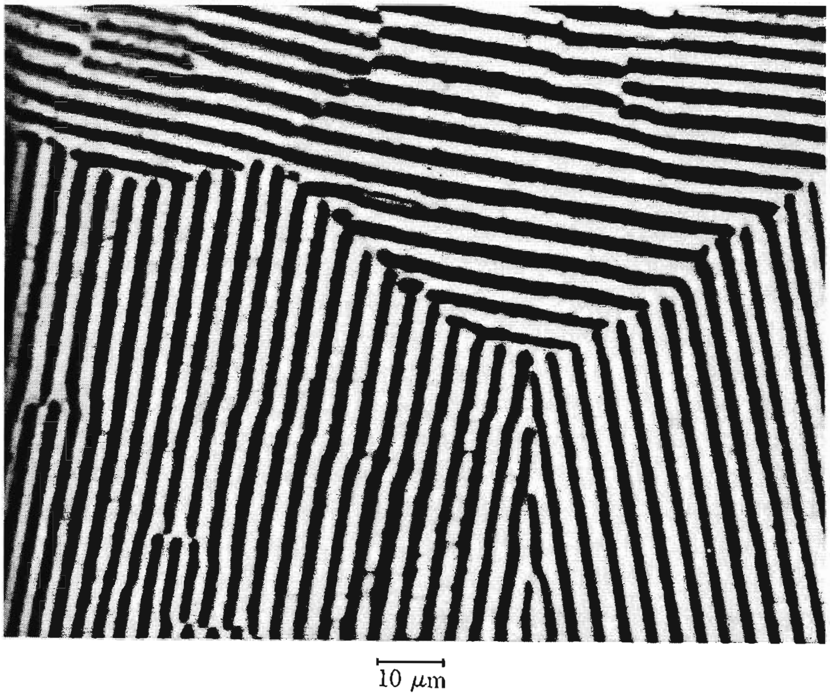

Figure 11 Microphotograph of the Pb-Sn eutectic. (Courtesy of J. D. Hunt and K. A. Jackson.)

The Au-Si eutectic is important in semiconductor technology because the eutectic permits low temperature welding of gold contact wires to silicon devices. Lead-tin alloys have a similar eutectic of $Pb_{0.26}Sn_{0.74}$ at 183°C. This or nearby compositions are used in solder: nearby if a range of melting temperatures is desired for ease in handling.

TRANSITION METAL ALLOYS

When we add copper to nickel, the effective magneton number per atom decreases linearly and goes through zero near $Cu_{0.60}Ni_{0.40}$, as shown in Fig. 12. At this composition the extra electron from the copper has filled the $3d$ band, or the spin-up and spin-down $3d$ sub-bands that were shown in Fig. 12.7b. The situation is shown schematically in Fig. 13.

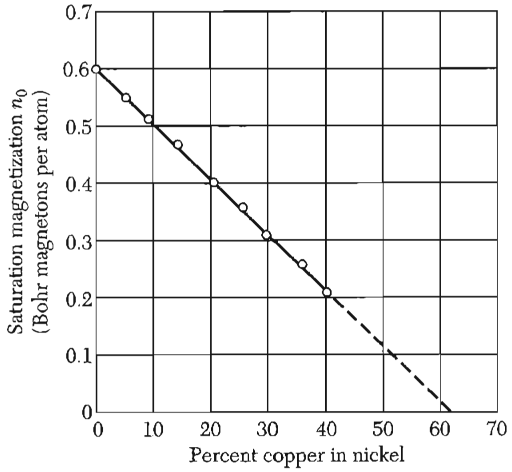

Figure 12 Bohr magneton numbers of nickel-copper alloys.

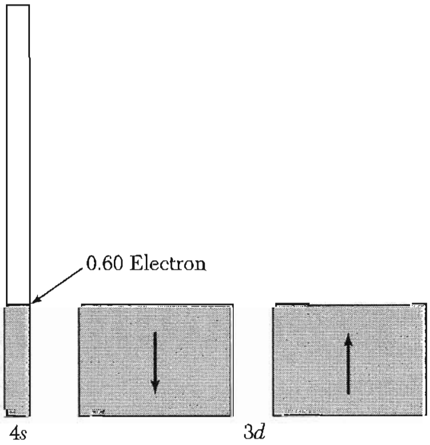

Figure 13 Distribution of electrons in the alloy 60Cu40Ni. The extra 0.6 electron provided by the copper has filled the d band entirely and increased slightly the number of electrons in the s band with respect to Fig. 12.7b.

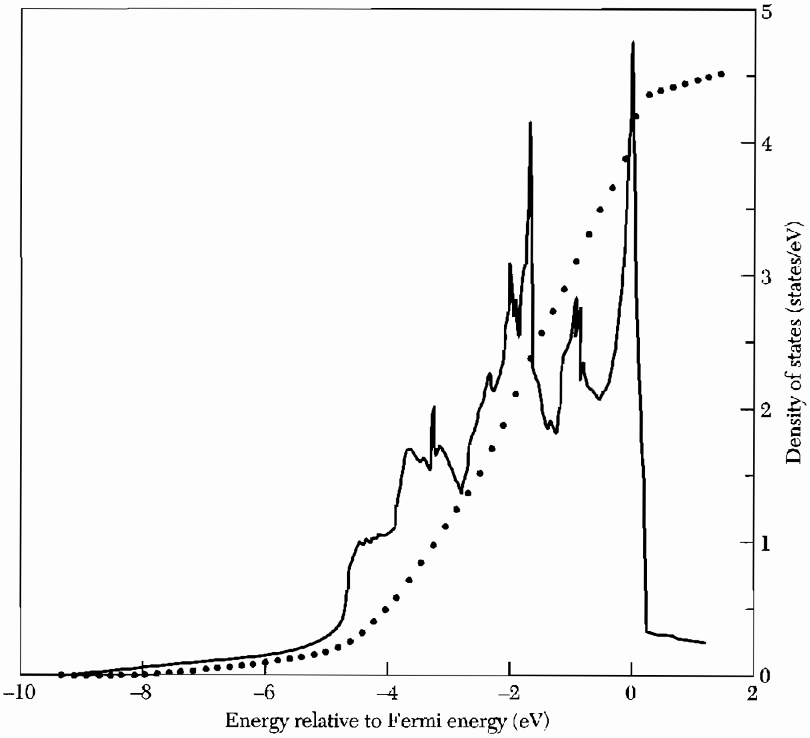

Figure 14 Density of states in nickel. (V. L. Moruzzi, J. F. Janak, and A. R. Williams.)

For simplicity the block drawings represent the density of states as uniform in energy. The actual density is known to be far from uniform; the result of a modern calculation is shown in Fig. 14 for nickel. The width of the $3d$ band is about 5 eV. At the top, where the magnetic effects are determined, the density of states is particularly high. The average density of states is an order of magnitude higher in the $3d$ band than in the $4s$ band. This enhanced density of states ratio gives a rough indication of the expected enhancement of the electronic heat capacity and of the paramagnetic susceptibility in the nonferromagnetic transition metals as compared with the simple monovalent metals.

Figure 15 shows the effect of the addition of small amounts of other elements to nickel. On the band model an alloying metal with z valence electrons outside a filled d shell is expected to decrease the magnetization of nickel by approximately z Bohr magnetons per solute atom. This simple relation holds well for Sn, Al, Zn, and Cu, with $z = 4, 3, 2$, and 1, respectively. For Co, Fe, and Mn the localized moment model of Friedel accounts for effective z values of -1, -2, and -3, respectively.

The average atomic magnetic moments of binary alloys of the elements in the iron group are plotted in Fig. 16 as a function of the concentration of

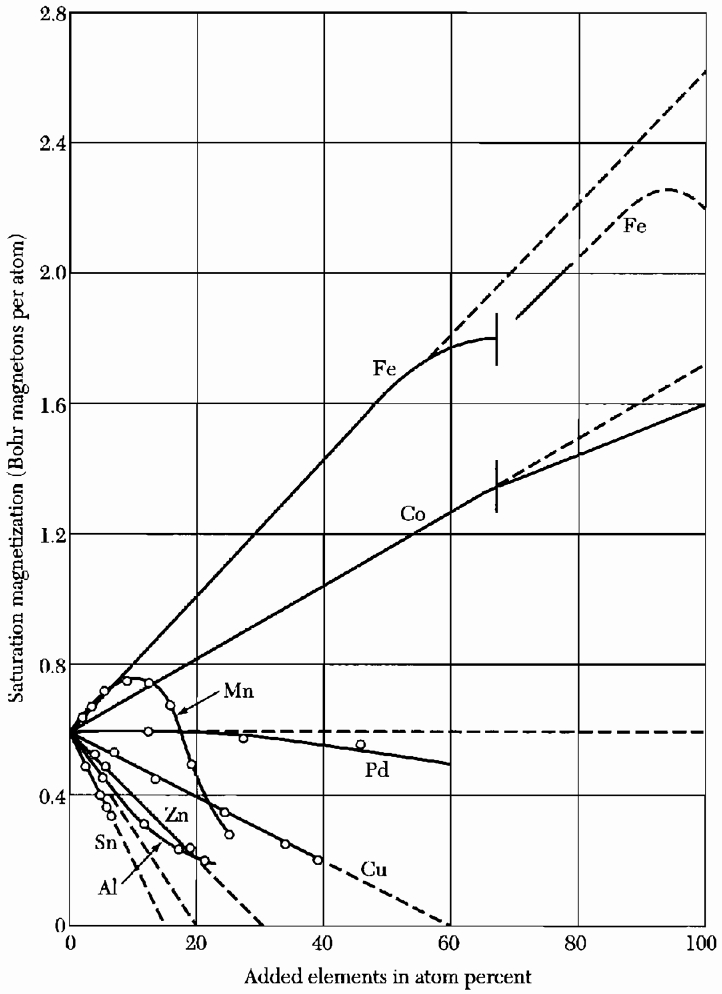

Figure 15 Saturation magnetization of nickel alloys in Bohr magnetons per atom as a function of the atomic percent of solute element.

electrons outside the $3p$ shell. This is called a Slater-Pauling plot. The main sequence of alloys on the right-hand branch follows the rules discussed in connection with Fig. 15. As the electron concentration is decreased, a point is reached at which neither of the $3d$ sub-bands is entirely filled, and the magnetic moment then decreases toward the left-hand side of the plot.

Electrical Conductivity. It might be thought that in the transition metals the availability of the $3d$ band as a path for conduction in parallel with the $4s$ band would increase the conductivity, but this is not the way it works out. The resistivity of the s electron path is increased by collisions with the d electrons; this is a powerful extra scattering mechanism not available when the d band is filled.

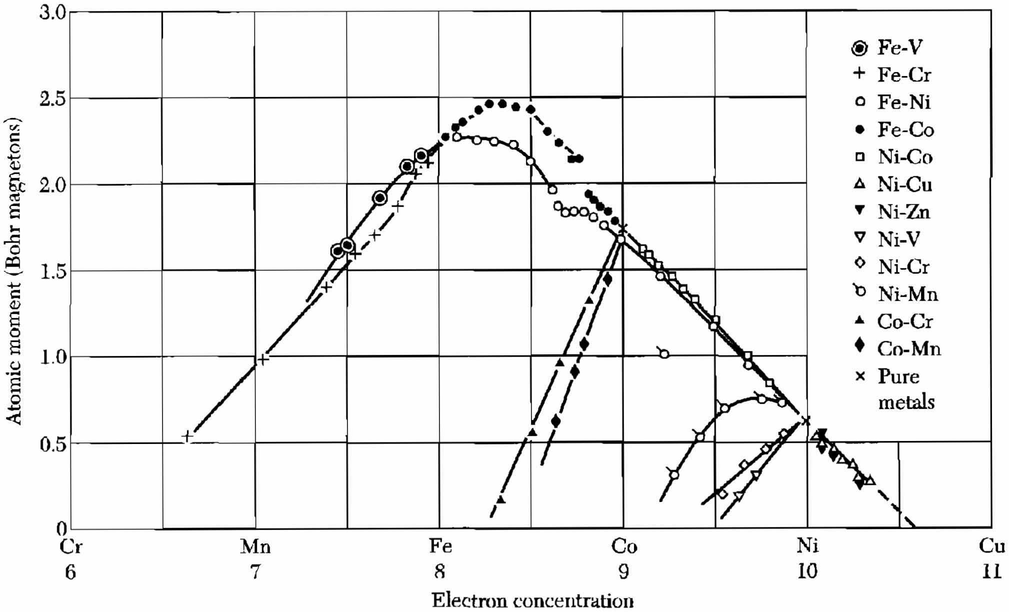

Figure 16 Average atomic moments of binary alloys of the elements in the iron group. (Bozorth.)

We compare the values of the electrical resistivities of Ni, Pd, and Pt in *microhm-cm* at 18°C with that of the noble metals Cu, Ag, and Au immediately following them in the periodic table:

Ni	Pd	Pt
7.4	10.8	10.5

Cu	Ag	Au
1.7	1.6	2.2

The resistivities of the noble metals are lower than those of the transition metals by a factor of the order of 5. This shows the effectiveness of the *s-d* scattering mechanism.

KONDO EFFECT

In dilute solid solutions of a magnetic ion in a nonmagnetic metal crystal (such as Mn in Cu), the exchange coupling between the ion and the conduction electrons has important consequences. The conduction electron gas is

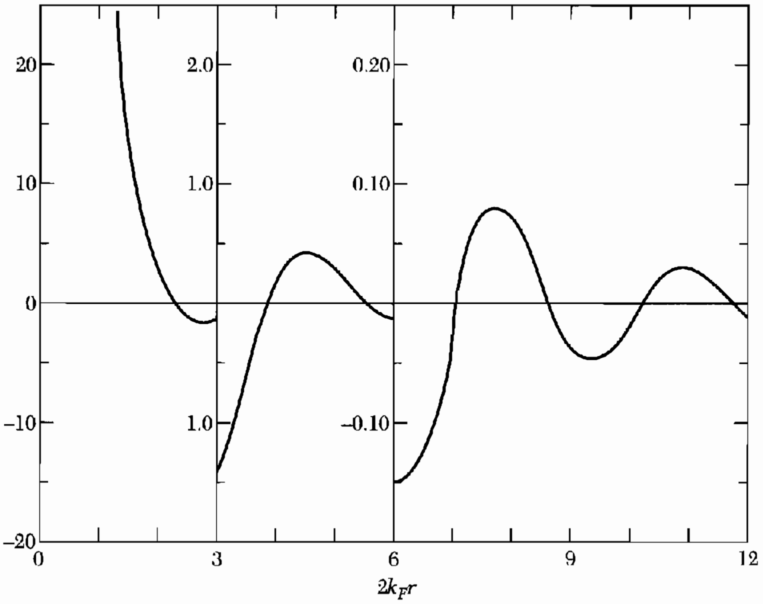

Figure 17 Magnetization of a free electron Fermi gas at $T = 0$ in neighborhood of a point magnetic moment at the origin $r = 0$, according to the RKKY theory. The horizontal axis is $2k_Fr$, where k_F is the wavevector at the Fermi surface. (de Gennes.)

magnetized in the vicinity of the magnetic ion, with the spatial dependence shown in Fig. 17. This magnetization causes an indirect exchange interaction[2] between two magnetic ions, because a second ion perceives the magnetization induced by the first ion. The interaction, known as the Friedel or RKKY interaction, also plays a role in the magnetic spin order of the rare-earth metals, where the spins of the 4*f* ion cores are coupled together by the magnetization induced in the conduction electron gas.

A consequence of the magnetic ion-conduction electron interaction is the **Kondo effect**, discussed in a different context in Chapter 18. A minimum in the electrical resistivity-temperature curve of dilute magnetic alloys at low temperatures has been observed in alloys of Cu, Ag, Au, Mg, Zn with Cr, Mn, and Fe as impurities, among others.

The occurrence of a resistance minimum is connected with the existence of localized magnetic moments on the impurity atoms. Where a resistance minimum is found, there is inevitably a local moment. Kondo showed that the anomalously high scattering probability of magnetic ions at low temperatures

[2] A review of indirect exchange interactions in metals is given by C. Kittel, Solid state physics **22**, 1 (1968); a review of the Kondo effect is given by J. Kondo, "Theory of dilute magnetic alloys," Solid state physics **23**, 184 (1969) and A. J. Heeger, "Localized moments and nonmoments in metals: the Kondo effect," Solid state physics **23**, 248 (1969). The notation RKKY stands for Ruderman, Kittel, Kasuya, and Yosida.

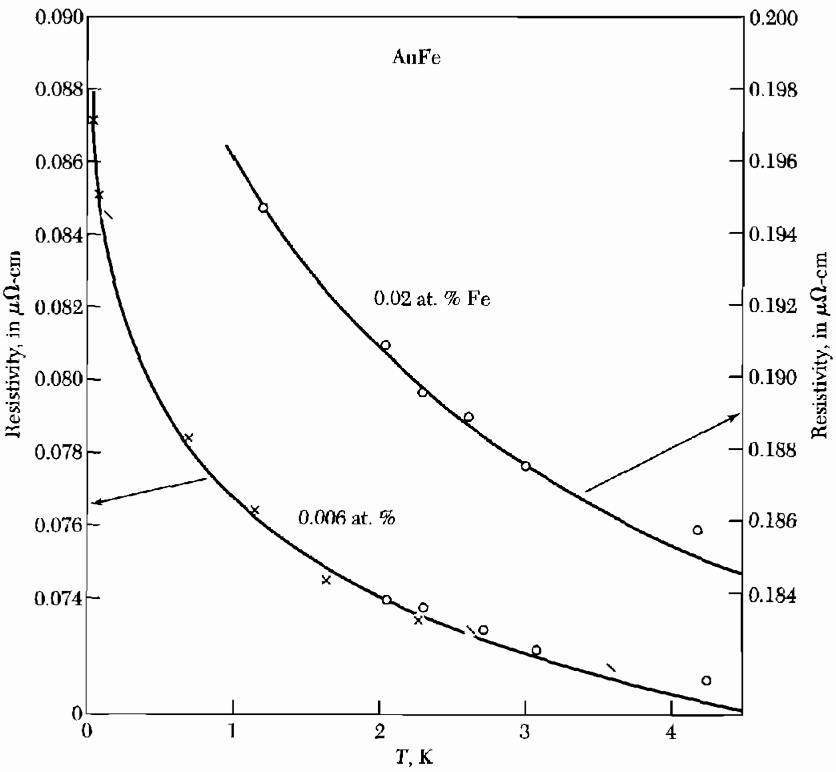

Figure 18 A comparison of experimental and theoretical results for the increase of electrical resistivity at low temperatures in dilute alloys of iron in gold. The resistance minimum lies to the right of the figure, for the resistivity increases at high temperatures because of scattering of electrons by thermal phonons. The experiments are due to D. K. C. MacDonald, W. B. Pearson, and I. M. Templeton; the theory is by J. Kondo. An exact solution was given by K. Wilson.

is a consequence of the dynamic nature of the scattering by the exchange coupling and of the sharpness of the Fermi surface at low temperatures. The temperature region in which the Kondo effect is important is shown in Fig. 18.

The central result is that the spin-dependent contribution to the resistivity is

$$\rho_{\mathrm{spin}} = c\rho_M \left[1 + \frac{3zJ}{\epsilon_F} \ln T \right] = c\rho_0 - c\rho_1 \ln T \ , \tag{12}$$

where J is the exchange energy; z the number of nearest neighbors; c the concentration; and ρ_M is a measure of the strength of the exchange scattering. We see that the spin resistivity increases toward low temperatures if J is negative. If the phonon contribution to the electrical resistivity goes as T^5 in the region of interest and if the resistivities are additive, then the total resistivity has the form

$$\rho = \alpha T^5 + c\rho_0 - c\rho_1 \ln T \ , \tag{13}$$

with a minimum at

$$d\rho/dT = 5aT^4 - c\rho_1/T = 0 \ , \tag{14}$$

whence

$$T_{\text{min}} = (c\rho_1/5a)^{1/5} \ . \tag{15}$$

The temperature at which the resistivity is a minimum varies as the one-fifth power of the concentration of the magnetic impurity, in agreement with experiment, at least for Fe in Cu.

Problems

1. ***Superlattice lines in Cu_3Au.*** Cu_3Au alloy (75% Cu, 25% Au) has an ordered state below 400°C, in which the gold atoms occupy the 000 positions and the copper atoms the $\frac{1}{2}\frac{1}{2}0$, $\frac{1}{2}0\frac{1}{2}$, and $0\frac{1}{2}\frac{1}{2}$ positions in a face-centered cubic lattice. Give the indices of the new x-ray reflections that appear when the alloy goes from the disordered to the ordered state. List all new reflections with indices ≤ 2.

2. ***Configurational heat capacity.*** Derive an expression in terms of $P(T)$ for the heat capacity associated with order/disorder effects in an AB alloy. [The entropy (8) is called the configurational entropy or entropy of mixing.]